INTEGRATED DESIGN, SIMULATION, AND EXPERIMENTAL MANUFACTURING OF AN AUTOMOTIVE WHEEL RIM

Tan Thong Ngo[1], Quoc Thai Pham[2]*, Quang Thach Bui[2]*, Trong Trinh Nguyen[2], Huu Truong Tran[2], Van Hoa Duong[3]

[1]*The University of Danang - University of Technology and Education, Vietnam*
[2]*The University of Danang - University of Science and Technology, Vietnam*
[3]*Duy Tan Univesity, Vietnam*

*Corresponding author: pqthai@dut.udn.vn; buithach03122003@gmail.com

(Received: April 26, 2026; Revised: June 10, 2026; Accepted: June 11, 2026)

DOI: 10.31130/ud-jst.2026.24(6A).253E

Abstract - This paper presents an integrated CAD/CAE/CAM-based methodology for the design and development of molds for automotive aluminum alloy wheel rims using the low-pressure die casting (LPDC) process. The study focuses on a 17-inch aluminum alloy wheel rim and integrates parametric CAD modeling, casting process simulation, mold design, and CAM-based machining preparation for mold cavity components. CAE simulations were conducted to evaluate mold filling behavior, temperature distribution, pressure evolution, air entrapment, and solidification characteristics in order to optimize the mold structure and improve casting feasibility. The simulation results indicate stable mold filling, favorable directional solidification behavior, and a reduced likelihood of casting defects such as shrinkage porosity and incomplete filling. The proposed workflow provides a practical digital framework for LPDC-oriented wheel rim and mold development, contributing to manufacturing optimization and engineering applications in modern automotive production.

Key words - CAD/CAE/CAM; Automotive Wheel Rim; Simulation; Low Pressure Die Casting; Creo Parametric Edu.

1. Introduction

The rapid growth of electric vehicles (EVs) worldwide, driven by increasing environmental concerns, advances in battery technology, and government policies promoting sustainable transportation, has significantly transformed the automotive industry [1, 2, 3]. In Vietnam, the EV market has also experienced remarkable expansion in recent years, supported by national green-transition initiatives and the emergence of domestic manufacturers [4]. As the demand for electric vehicles continues to rise, the need for lightweight, durable, and high-performance automotive components becomes increasingly important. In modern automotive manufacturing, wheel rims are critical structural components that directly influence vehicle safety, performance, and durability. Conventional design approaches often require long development cycles and repeated prototyping, making it difficult to simultaneously optimize lightweight characteristics and mechanical strength.

With the advancement of digital engineering technologies, CAD/CAE/CAM tools enable more efficient wheel rim design, simulation, and manufacturing. These technologies support the evaluation of structural behavior, material performance, and manufacturability prior to physical production, thereby reducing development time and prototyping costs.

Recent trends in digital manufacturing have increasingly emphasized integrated product development, in which design, simulation, and manufacturing are interconnected within a unified workflow. Unlike conventional standalone CAD/CAE/CAM applications, the present study proposes an integrated LPDC-oriented methodology for aluminum alloy wheel rim development. The proposed workflow combines parametric wheel design, casting simulation, mold development, manufacturability analysis, and CNC machining preparation within a closed-loop digital framework to improve casting quality and reduce redesign iterations before manufacturing.

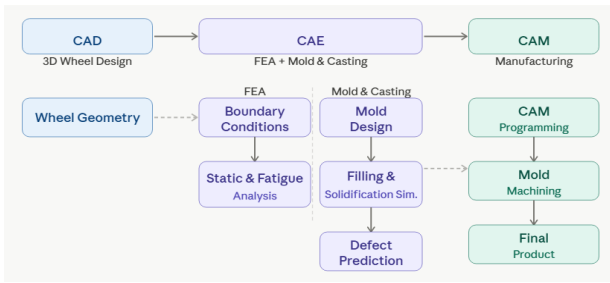

Figure 1. *Integrated CAD–CAE–CAM process flow for wheel design and manufacturing*

The process combines wheel geometry design, structural and casting simulation, mold design, defect prediction, and CAM-based machining preparation for mold cavity manufacturing within a unified digital framework. This integrated approach enables early evaluation of wheel performance and casting behavior, thereby improving manufacturability and reducing potential casting defects prior to production.

2. Materials and methods

2.1. Wheel rim design

2.1.1. Determination of the profile parameters of an automotive wheel rim

The wheel rim was modeled in Creo Parametric Edu and has a geometric configuration with six spokes [5]. The key design parameters include:

- Rim diameter: 17 inches (431.8 mm);
- Rim width: 7.5 inches (190.5 mm);
- Rim thickness: 6 mm.

Parametric modeling allowed flexible control of spoke thickness, curvature, and offset distance, thereby

facilitating optimization studies. Fillet radii were adjusted to minimize stress concentration while maintaining aesthetic appeal. According to ISO 3911 [6] and SAE J2530 [7] standards, the rim profile is defined by several geometric elements that ensure compatibility between the rim and tire bead, as well as proper air sealing.

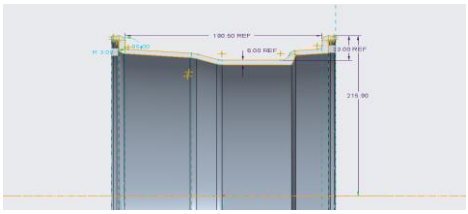

Figure 2. *Wheel rim profile showing the main geometric parameters*

2.1.2. Hub and spoke profile modeling

The spokes play a dual role: they transfer radial, lateral, and tangential forces while also contributing to the wheel's visual design. The rim features six spokes that symmetrically connect the hub and the outer rim flange.

Each spoke was generated from a 3D guide curve created between the hub and rim using loft and sweep operations. The curvature of the spokes was optimized to achieve a smooth transition, thereby reducing peak stress at the junctions [8].

- Spoke thickness: 30 mm;
- Spoke width: 60 mm;
- Angle of inclination of spokes: 18°.

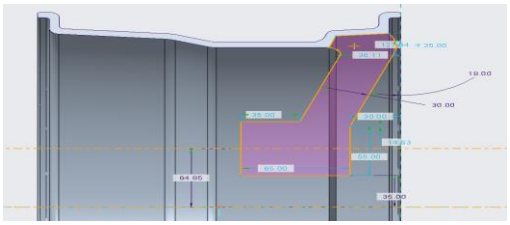

Figure 3. *Spoke geometry*

The hub section serves as the interface connecting the wheel to the vehicle axle. The main geometric parameters were defined based on the target vehicle's mounting configuration and brake system dimensions [9,10].

- Bolt circle diameter (PCD): 129.7 mm;
- Number of bolt holes: 6 × Ø14 mm.

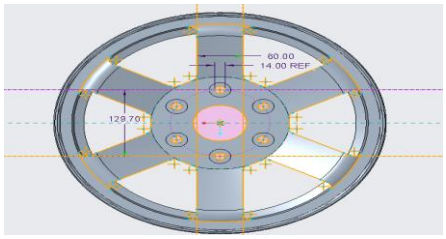

Figure 4. *Wheel axle design*

2.1.3. Wheel design results

Figure 5. *Wheel design result*

2.2. Selection of materials and casting methods

2.2.1. Material selection

Wheel rims constitute critical automotive components that must endure substantial mechanical loads as well as diverse environmental influences throughout both operational service and manufacturing processes. Consequently, the selected material is required to satisfy stringent criteria, including high mechanical strength, fatigue resistance, impact resistance, dimensional stability under thermal variations, and durability against corrosion and wear. These properties collectively ensure that the rim not only maintains structural integrity and operational safety during vehicle service but also supports efficient and reliable production in modern industrial environments [11].

- High mechanical strength, fatigue resistance and impact resistance.
- Lightweight and corrosion-resistant characteristics.
- Good castability and machinability.

Conclusion: A356 aluminum alloy represents a balanced choice in terms of weight, strength, castability, and corrosion resistance, making it suitable for general automotive wheel rims.

Table 1. *Material properties of A356 aluminum alloy*

Property	Value	Unit
Density	2.68	g/cm³
Ultimate tensile strength	220–310	MPa
Yield strength	160–240	MPa
Elongation	3–8	%
Elastic modulus	71	GPa
Thermal conductivity	151	W/m·K
Melting temperature range	555–615	°C
Hardness	70–80	HB
Corrosion resistance	Good	-
Castability	Excellent	-

2.2.2. Selection of casting method

Low-pressure die casting (LPDC) is a casting method that uses low compressed-air pressure to force molten metal from the furnace into the die cavity, allowing the metal to continuously fill the mold and produce components with high dimensional accuracy, uniform microstructure, and minimal casting defects. This method is widely used for aluminum alloy components.

Advantages:

- Smooth metal flow, minimizing air entrapment and porosity.
- Excellent shrinkage compensation during solidification.
- High and uniform mechanical properties.
- Complete filling of intricate mold features, resulting in improved surface quality and reduced machining requirements.
- Low defect rate and stable production process.

2.3. Designing molds for car wheel rims

2.3.1. Design process

The mold design strategy was developed considering the complex geometry of the aluminum alloy wheel rim in

order to improve casting quality, production efficiency, dimensional quality, and surface aesthetics during the low-pressure die casting (LPDC) process.

Appropriate draft angles and surface finishing conditions were considered for the spokes and rim regions to facilitate mold release while minimizing the risk of surface deformation and casting defects. A draft angle of approximately 3° relative to the mold opening direction was applied to the vertical surfaces to ensure smooth ejection of the casting from the mold cavity.

For the mold material, H13 tool steel was selected due to its high mechanical strength, excellent thermal fatigue resistance, and suitability for high-temperature operating conditions commonly encountered in LPDC applications.

a. Mold design

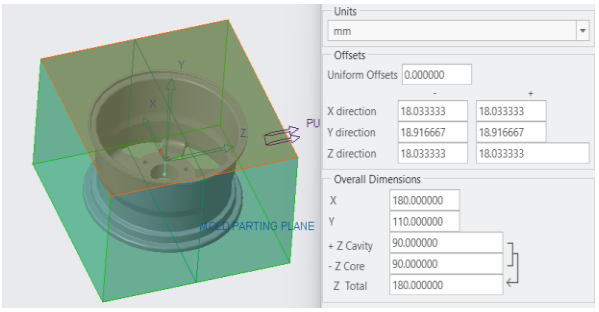

Figure 6. *Setting the overall dimensions of the mold*

b. Shrinkage by scale

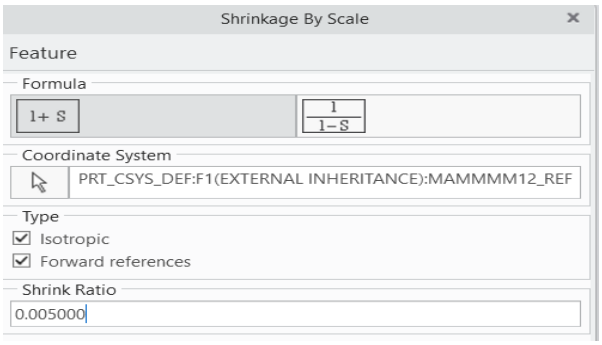

Figure 7. *Set the shrinkage by scale*

A shrinkage by scale value of 0.005 was applied in the mold design to compensate for the dimensional contraction of the A356 aluminum alloy during solidification and cooling in the low-pressure die casting (LPDC) process. This value helps maintain the dimensional accuracy of the wheel rim after casting and reduces the risk of geometric deviation caused by thermal shrinkage.

c. Parting surface

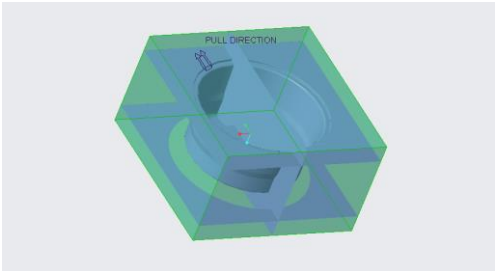

Figure 8. *Parting surface*

d. Volume split

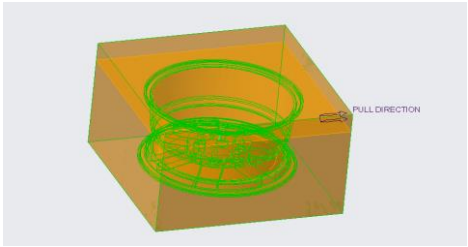

Figure 9. *Execute command volume split*

e. Mold result

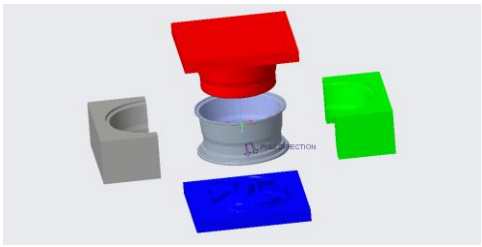

Figure 10. *Mold opening results*

2.4. Setting boundary conditions to simulate the strength of a car wheel rim using Cad/Cam software

2.4.1. Material Properties and Boundary Conditions

a. Material properties

The material selected for this study is A356-T6 aluminum alloy, a heat-treated cast aluminum widely utilized in the automotive industry. This alloy is the industrial standard for wheel rim manufacturing due to its exceptional strength-to-weight ratio, superior castability, and high mechanical durability. The T6 heat treatment further enhances the material's yield strength and hardness, ensuring the structural integrity of the wheel under rigorous operational conditions.

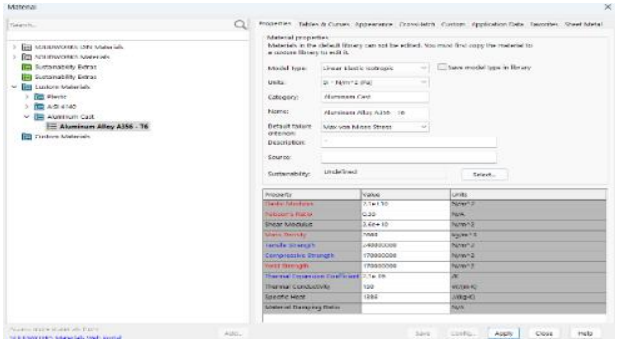

Figure 11. *Material specifications table for Aluminum Alloy A356 – T6*

Table 2. *S–N fatigue curve data table*

Points	N (No. of Cycles)	S (Stress – MPa)
1	10,000	160
2	100,000	120
3	1,000,000	90
4	10,000,000	70
5	100,000,000	55

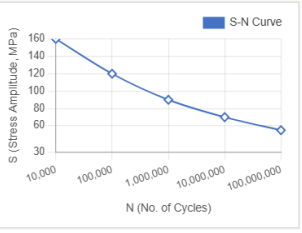

b. Boundary conditions

To accurately replicate the operational environment of the wheel rim, external loads are calculated based on the total vehicle weight (m) and gravitational acceleration

(g). The static load per wheel (F_{bx}) is determined by the following expression [12]:

$$F_{bx} = \frac{mg}{4} \quad (1)$$

To account for extreme operating conditions, such as sudden braking, rapid acceleration, or navigating uneven terrain – a dynamic coefficient ranging from 1.5 to 3.0 is incorporated ($k = 2$). Consequently, the final design load is defined as follows:

$$F_{bx} = k\frac{mg}{4} \quad (2)$$

- Total vehicle weight: $m = 2200(kg)$;

- Gravitational acceleration: $g = 9.81$.

The design load applied to the wheel rim was determined to be 10,791 N.

2.5. Casting simulation setup

2.5.1. Material selection

The material properties and corresponding simulation parameters were defined prior to the casting simulation.

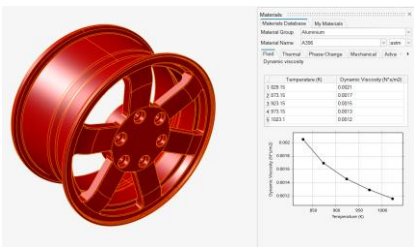

Figure 12. *Viscosity chart of material*

2.5.2. Gravity direction setup

The gravity direction was defined from top to bottom, perpendicular to the plane of the wheel spokes.

Figure 13. *Gravity direction setup*

2.5.3. Gate location setup

For symmetrical circular products such as wheel rims, an axial or centrally symmetric gate design is commonly recommended. According to casting design principles reported in Campbell and the ASM Handbook, this configuration enables uniform pressure distribution and stable molten metal flow, thereby ensuring complete mold filling and minimizing casting defects such as air entrapment and misrun [13].

The following parameters were calculated using the simulation software:

- Volume of filled metal.

$V = 3.827 \times 10^6 (mm^3)$

- Estimated fill time.

$t = 5(s)$

- Metal flow rate through the gate.

$v_{gate} = 500(mm/s)$

Metal flow [14]:

$$Q = \frac{V}{t} \quad (3)$$

Cross- sectional area of the gate [14]:

$$A_{gate} = \frac{Q}{v_{gate}} \quad (4)$$

Gate diameter [14]:

$$D = \sqrt{\frac{4A_{gate}}{\pi}} \quad (5)$$

Based on the calculated flow conditions, the gate diameter was determined to be 44.16 mm.

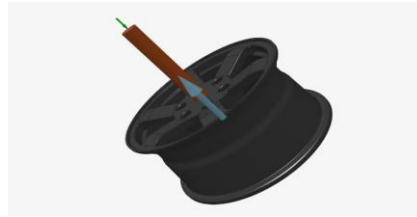

Figure 14. *Gate location setup*

2.5.4. Mold setup

A356 aluminum alloy is widely used for manufacturing automotive wheel rims, while H13 hot-work tool steel is commonly selected for low-pressure die casting molds due to its excellent thermal fatigue resistance and high-temperature mechanical properties [15].

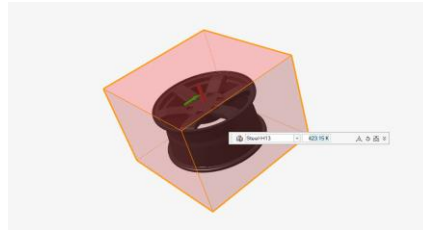

Figure 15. *Mold setup*

2.5.5. Selection of casting method and parameter setup

The simulation parameters used for the LPDC process are listed as follows:

- Density of liquid metal.

$\rho = 2.398\ kg/m^3$

- Gravitational acceleration.

$g = 9.8\ m/s^2$

- Runner height.

$h_1 = 0.6\ m$

- Total casting height.

$h_2 = 0.82\ m$

- Initial pressure [16]:

$$P_j = \rho g h_1 \quad (6)$$

The initial filling pressure was determined to be $14100.24 Pa$

- Late stage pressure [16]:

$$P_f = \rho g h_2 \quad (7)$$

The late-stage pressure was determined to be $19188.08 Pa$

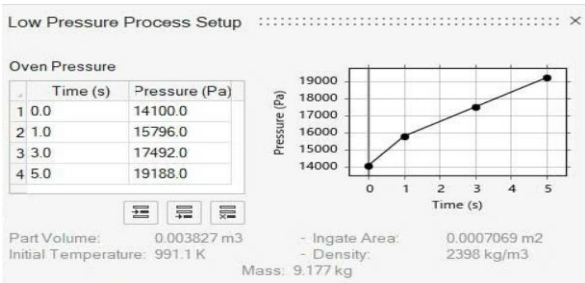

Figure 16. *Technical specifications for the low-pressure die casting process*

Table 3. *Summary of LPDC simulation parameters and input conditions*

Parameter	Symbol	Value	Unit
Casting alloy	-	A356	-
Mold material	-	H13	-
Gate diameter	D	44.16	mm
Gravitational acceleration	g	9.8	m/s²
Density of liquid metal	ρ	2398	kg/m³
Runner height	h_1	0.60	m
Total casting height	h_2	0.82	m
Initial pressure	P_1	14,100.24	Pa
Final pressure	P_2	19,188.08	Pa

3. Simulation results and discussion

3.1. Static and fatigue analysis results and discussion

3.1.1. Static analysis results

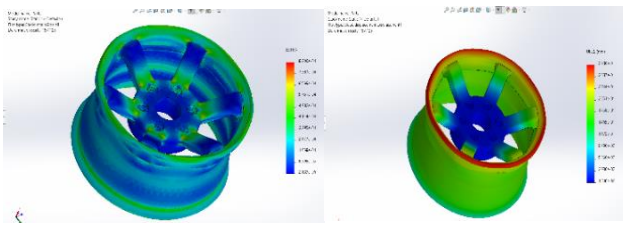

Figure 17. *Results of static structural analysis of the wheel rim*

The static structural simulation results were evaluated using the von Mises stress criterion. The maximum stress obtained from the Cad/Cam simulation was approximately 72.5 MPa, which is significantly lower than the yield strength of A356-T6 aluminum alloy (170 MPa). The calculated safety factor was approximately 2.34, indicating that the wheel rim satisfies the strength requirement under static loading conditions. High-stress regions were mainly concentrated at the spoke roots, bolt-hole areas, and the connection between the spokes and hub due to stress concentration effects. The maximum total deformation was approximately 0.293 mm and occurred mainly at the outer rim region. This relatively small displacement demonstrates good structural stiffness and deformation resistance of the wheel rim design.

3.1.2. Fatigue analysis results

The fatigue analysis results indicate that the wheel rim possesses high fatigue durability under the applied cyclic loading conditions. The predicted fatigue life ranged from approximately 3.67×10^6 to 1.0×10^8 cycles, with most regions exhibiting very high fatigue life. These results demonstrate that the proposed wheel rim design satisfies the fatigue-strength requirements for practical automotive applications.

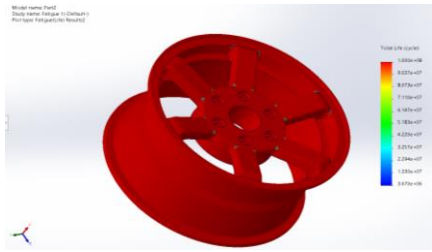

Figure 18. *Fatigue life distribution of the wheel rim*

3.2. Simulation results of the casting process using the low-pressure casting method

3.2.1. Filling simulation results

a. Filling temperature

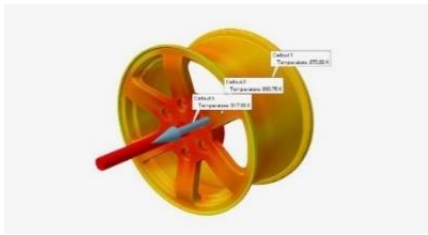

Figure 19. *Select three locations for evaluation*

We monitor temperatures at three critical locations: the wheel rim, the wheel hub and the axle interface.

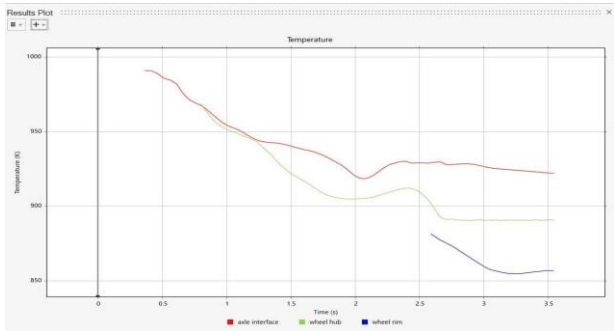

Figure 20. *Temperature evolution during the filling stage*

As illustrated in the temperature distribution results, the axle interface region retained the highest temperature during the filling stage, reaching approximately 922.04 K due to its larger wall thickness and slower cooling rate. The wheel hub region exhibited an intermediate temperature of approximately 890.81 K, while the wheel rim region cooled more rapidly to approximately 856.95 K because of its thinner geometry and larger heat dissipation surface area.

The temperature evolution curves further confirm this thermal behavior. The axle interface region maintained a relatively stable temperature range of approximately 920–930 K throughout the filling process, whereas the wheel hub temperature gradually decreased to approximately 890–910 K. In contrast, the wheel rim region experienced the fastest cooling rate, with temperatures decreasing to approximately 855–860 K near the end of filling. The

temperature difference between the axle interface and wheel rim regions reached approximately 60–70 K, promoting favorable directional solidification from the outer rim toward the central hub and gate regions.

No abrupt temperature fluctuations or thermal instabilities were observed during the filling stage, indicating stable molten metal flow conditions and a low probability of turbulence-related casting defects such as air entrapment and incomplete filling.

b. Filling time

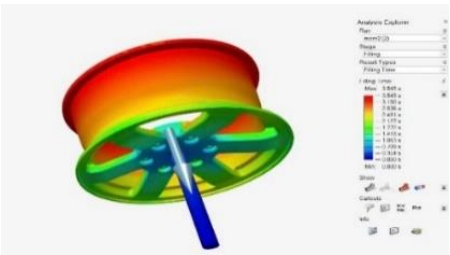

Figure 21. *Filling time*

The simulation results in Figure 21 indicate a stable filling process for the 17-inch wheel using the LPDC method. The molten A356 alloy follows a strict bottom-up sequence, starting from the center hub at 0.709 s, progressing through the spokes, and completing at the upper rim with a total time of 3.545 s. This steady filling rate maintains a laminar flow regime, effectively minimizing air entrainment and reducing the risk of misrun defects.

c. Pressure of filling process

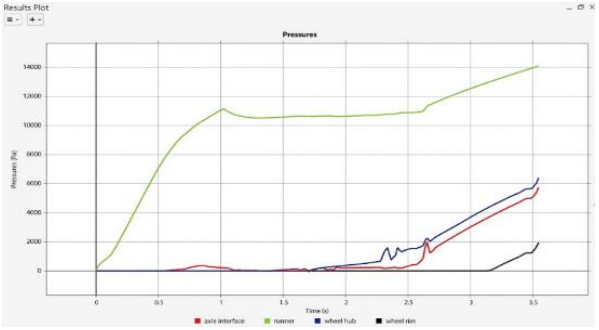

Figure 22. *Pressure evolution during the filling stage*

As shown in Figure 22, the runner pressure (green) rises to 11,000 Pa within 1.0 s to initiate the flow, then plateaus at 10,500 Pa to ensure a consistent filling velocity. The pressure at the wheel hub (blue) and rim (black) remains negligible until the metal reaches these zones at 2.2 s and 3.1 s, respectively. At the conclusion of the process (3.5 s), the pressure across all regions increases to a peak of 14,000 Pa, which enhances feeding efficiency during the early stages of solidification.

d. Last air

The Last Air simulation results reveal that the air within the mold is progressively displaced toward the rim edges, which are the final areas to be filled in the low-pressure die casting process. The air entrapment distribution is consistent with the bottom-up and inside-out filling patterns. However, an appropriate venting system must be integrated into these zones to mitigate the risk of gas porosity and enhance the overall casting quality [17].

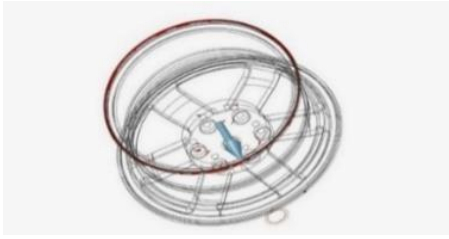

Figure 23. *Last air*

3.2.2. Solidification simulation results

a. The temperature of the solidification process

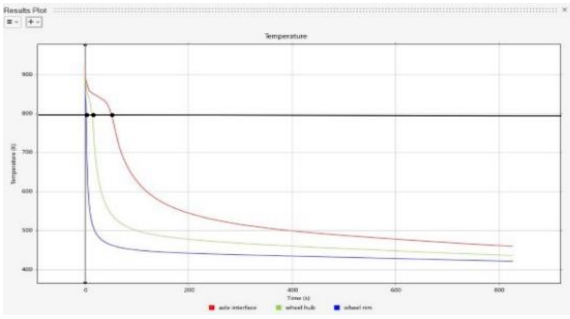

Figure 24. *Temperature evolution during solidification*

The temperature evolution curves in Figure 24 provide a quantitative basis for the thermal distribution analysis. The wheel rim (blue curve) exhibits the most rapid cooling rate, with the temperature dropping from approximately 850 K to 450 K within the first 50 seconds. In contrast, the wheel hub (green curve) and the axle interface (red curve) retain heat significantly longer, taking approximately 150 seconds and 300 seconds, respectively, to reach the same 500 K threshold. This temperature gradient confirms a directional solidification pattern from the periphery to the center, which is essential for ensuring effective metal feeding and mitigating shrinkage defects [18].

b. Solidification time

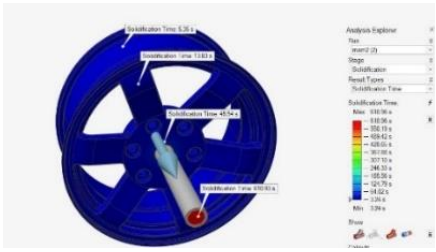

Figure 25. *Solidification time*

Table 4. *LPDC casting simulation results for A356 aluminum alloy wheel*

Evaluated parameter	Value	Unit
Axle interface temperature range	920–930	K
Wheel hub temperature range	890–910	K
Wheel rim temperature range	855–860	K
Total mold filling time	3.545	s
Initial runner pressure	11,000	Pa
Stable filling pressure	10,500	Pa
Maximum pressure at final filling stage	14,000	Pa
Rim solidification time	5.35	s
Spoke solidification time	13.83	s
Hub solidification time	45.54	s

The simulation of solidification time, as illustrated in Figure 25, reveals a well-defined solidification sequence that aligns with LPDC feeding principles. Quantitative data from the specific callouts show that the outer rim solidifies first at 5.35 s, followed by the spokes at 13.83 s, and the central hub at 45.54 s. The final region to solidify is the riser/sprue, with a maximum duration of 610.93 s. This extended solidification time at the gate area ensures that sustained pressure is applied throughout the process, effectively minimizing shrinkage porosity in the heavy-walled sections of the wheel.

3.3. Mold manufacturing results

The research team first established the structural configuration of the mold core assembly. After the mold separation process, specialized computer-aided manufacturing (CAM) software was utilized to generate precise machining toolpaths. Subsequently, the mold core machining process was simulated within an integrated CAD/CAM environment to verify machining feasibility and optimize the manufacturing parameters, as illustrated in Figure 26 [19, 20].

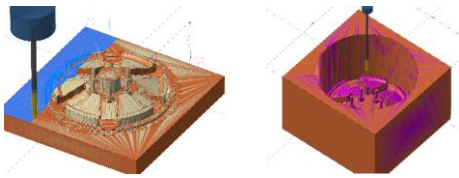

Figure 26. *Simulating toolpath in Mastercam edu*

The workpiece was set up and the NC program was installed on a 3-axis CNC milling machine to perform the machining process, as shown in Figure 27.

Figure 27. *Machining of mold cage structures*

Figure 28. *Mold cavities for automobile wheel casting after complete CNC machining*

4. Conclusion

This study presented an integrated CAD/CAE/CAM-based workflow for the design, simulation, and manufacturing preparation of aluminum alloy automotive wheel rims using the low-pressure die casting (LPDC) process. The proposed methodology combined parametric wheel design, casting simulation, mold development, and CNC machining preparation within a unified digital framework.

The CAE simulation results indicated stable mold filling behavior, favorable solidification characteristics, and a reduced risk of casting defects such as shrinkage porosity and incomplete filling. In addition, the CAM-based machining preparation demonstrated the feasibility of manufacturing the mold cavity components using CNC machining processes.

The proposed workflow provides a practical foundation for LPDC-oriented wheel rim and mold development and can support future experimental casting and manufacturing optimization studies.

REFERENCES

[1] P. Q. Thai, V. C. Tai, H. D. Tri, and V. T. Nam, "A Study of Converting a Conventional Vehicle into an Electric Vehicle," *Int. J. Mech. Eng. Robot. Res.,* pp. 569–574, 2022, doi: 10.18178/ijmerr.11.8.569-574.

[2] D.-Q. Vo, T. Q. Pham, D. L. Luu, D. Q. Hung, P. V. Quy, and P. H. Truyen, "Comparative CFD analysis of natural and forced convection cooling for VinFast VF3 battery in tropical urban conditions," *UD-JST*, vol. 23, no. 10B, pp. 42–46, Oct. 2025.

[3] P. Q. Thai and H. D. Tri, "Modeling and simulation of the powertrain of electric vehicles," *UD-JST*, vol. 19, no. 4.1, pp. 47–52, Apr. 2021.

[4] Pham QT, Huynh DT, Bui VG, Phan VB, "Application of Edge Detection Algorithm for Self-Driving Vehicles," *2022 7th National Scientific Conference on Applying New Technology in Green Buildings (ATiGB), Da Nang, Vietnam,* 2022, pp. 225-228, doi: 10.1109/ATiGB56486.2022.9984117.

[5] International Organization for Standardization, "*Passenger car tyres and rims (metric series)- Part 1: Tyres*," ISO 4000-1: 2015, 2015.

[6] International Organization for Standardization, "*Wheels and rims for pneumatic tyres – Vocabulary, terminology and definitions*," ISO 3911:2012, 2012.

[7] SAE International, "*Wheels – Passenger Car and Light Truck Performance Requirements and Test Procedures*," SAE J2530, 2019.

[8] International Organization for Standardization, "*Road vehicles- Wheels/ rims for passenger cars- Test methods*," ISO 3006: 2015, 2015.

[9] Ministry of Transport, "*National technical regulation on light alloy wheels for automobiles*," QCVN 78:2014/BGTVT, Hanoi, 2014.

[10] International Organization for Standardization, "*Road Vehicles- Metric series wheel- Mounting holes and nut seats- Dimensions*," ISO 4107: 2006, 2006.

[11] M. F. Ashby and K. Johnson, *"Materials and Design: The Art and Science of Material Selection in Product Design*," 3rd ed., Oxford, UK: Butterworth- Heinemann, 2014.

[12] N. K. Trai and N. T. Hoan, "*Automobile Structure*". Hanoi, Vietnam: Transport Publishing House, 2008.

[13] J. Campbell, *Complete Casting Handbook: Metal Casting Processes, Metallurgy, Techniques and Design*, 2nd ed. Oxford, UK: Elsevier Butterworth-Heinemann, 2015.

[14] ASM International, *ASM Handbook, Volume 15: Casting*. Materials Park, OH, USA: ASM International, 2008.

[15] ASM International*, ASM Handbook, Volume 1: Properties and Selection-Irons, Steels, and High-Performance Alloys.* Materials Park, OH, USA: ASM International, 1990.

[16] R. W. Fox, A. T. McDonald, and P. J. Pritchard*, Introduction to Fluid Mechanics*, 7th ed. Hoboken, NJ, USA: John Wiley & Sons, 2011.

[17] N. T. Thong, N. T. Tranh, "*Design and manufacture of molds with Creo 2.0,"* Transport Publishing House, 2005.

[18] J. K. Kittur, G. C. M. Patel, and M. B. Parappagoudar, "Modeling of pressure die casting process: An artificial intelligence approach," *International Journal of Metalcasting,* vol. 10, no. 1, pp. 70–87, 2016, doi: 10.1007/s40962-015-0001-7.

[19] Mastercam, "CAD/CAM Products & Solutions" *www.mastercam.com*, 2026. [Online]. Available: https://www.mastercam.com/solutions/products/. [Accessed: Jan. 28, 2026].

[20] B. T. M. Tu, P. Q. Thai, N. T. Thong, N. L. C. Thanh, and T. M. Truong, "Study on applying the multitasking controller H7K-A to CNC Router machines for teaching and scientific research at the University of Danang," *UD-JST*, vol. 22, no. 7, pp. 12-16, 2024.